Designing the Wood Foam Core for Manufacturing of Lightweight Sandwich Structure Engineered Wood

Utai Meekum,* and Waree Wangkheeree

Wood foam cores manufactured from *Eucalyptus* fiber/epoxy adhesive and 4,4' oxybis(benzene sulfonyl hydrazide) (OBSH), ethyl acetate (EA), and microsphere polymer bead (Expancel®) as foaming agents were investigated. A 10 phr of OBSH showed superior properties of the 0.50 g/cm^3 wood foam and that 0.70 g/cm^3 was the optimal density. Also, 17 phr of EA loading gave rise to the better mechanical properties and was considered the optimal content. The microsphere polymer bead did not achieve significant expansion under the conditions employed. Manufacturing of single (X1) and double (X2) layer of lightweight sandwich structures engineered woods with teak/glass fiber-reinforced polymer (GFRP) skins was studied. The enhancement of the sandwich structures' properties was mainly contributed by the core and also by the added thin interlaminated GFRP layer. In X1 and X2 sandwich structures, with the same volume fraction of core(s), marginal improvement occurred in the properties, caused by the addition of the thin inter-layer of GFRP. Small contributions of the core properties on the sandwich structures were also demonstrated. The sandwich structure derived from the OBSH core was superior in mechanical properties and heat distortion temperature (HDT). The sandwich structure made from EA was unsuccessful in achieving water resistance.

Keywords: Foaming agents; Wood foam; Lightweight sandwich structure; Engineered wood

*Contact information: School of Design Technology, Institute of Engineering, Suranaree University of Technology, Maung, Nakorn Ratchasima, Thailand; *Corresponding author: umsut@g.sut.ac.th*

INTRODUCTION

Sandwich structures have been used in a wide range of engineering applications, such as transportation vehicles, boat hulls, and space structures, due to their light weight, and high stiffness to weight ratio, *etc*. (Vaikhanski and Nutt 2003; Fang *et al*. 2015; Mohamed *et al*. 2015). Most high performance structural foams are made by expanding and blowing liquid polymers to form rigid, low-density foams that are thermoplastic and made of partly cross-linked polyvinyl chloride (PVC) (Vaikhanski and Nutt 2003). The foam materials made from thermoplastic reinforced with fiber were attempted, such as poly(propylene)(PP)/wood flour composites and surface modified rice husk filled polyvinylchloride (Kedar *et al.* 2011; Chand *et al*. 2012; Soares and Nachtigall 2013).

Wood/natural rubber composite and ethylene-propylene diene rubber (EPDM) foam made *via* the compression molding technique have been reported (Yamsaengsung and Sombatsompop 2009). Two different forms of 4,4'oxybis(benzenesulfonylhydrazide) (OBSH) blowing agent were used: pure OBSH and ethylenepropylene-bound-OBSH (EPR–b-OBSH). The EPR–b-OBSH gave the EPDM foam a greater number of cell structures. However, it had worse elastic recovery compared to OBSH due to the deformation of cell structures after prolonged compression loading (Yamsaengsung and

Sombatsompop 2009). Moreover, the thermosetting foam that was epoxy-based was also studied (Mazzon *et al.* 2015). Highly reactive epoxy foams were obtained by mixing epoxidized plant-oil-derivatives with a cycloaliphatic amine hardener and a harmless foaming agent, sodium bicarbonate $NaHCO_3$ (SB). It was possible to produce the foams within a few minutes with good thermal and apparent density.

Engineered woods, particularly the sandwich-type containing a high performance foam core, would be interesting candidates for such a material with high strength and light weight. Recently, a study on the effect of the skin, core, and core thickness on the mechanical strength of lightweight panels was attempted. The mechanical strength of lightweight panels made with a polyurethane foam core was better than that of lightweight panels made with a kraft paper honeycomb core (Pishan *et al.* 2014). As an alternative, the production of lightweight sandwich panels using preformed hardwood veneer residue/polyurethane foam cores and different wood veneers as face layers was reported. Their obtained results demonstrated the viability of the newly developed panels for both structural and non-structural applications (Denes *et al*. 2008). The natural composite roof for housing application, structural panels, and unit beams were manufactured from soybean oil-based resin and natural fibers using vacuum assisted resin transfer molding (VARTM). The physical, chemical, and mechanical outcomes of the beams yielded good results in line with desired structural performance (Dweib *et al*. 2004). A new type of hybrid composite sandwich wall panel with two different types of natural fibers reinforced plastics (NFRP) laminate was incorporated into the new sandwich panel as an intermediate layer was explored. Three levels of a factor have been examined. The results showed that the incorporation of an intermediate layer significantly enhanced the load carrying capacity of the sandwich panels (Fajrin *et al*. 2013).

Investigations of the fracture toughness of PVC foams used as sandwich core materials and studies of the micromechanical modelling of closed-cell polymeric foams in the sandwich structures have been published (Poapongsakorn and Carlsson 2013; Chen *et al.* 2015). The influence of the formulation variables of wood flour-reinforced phenolic foams (WRPFs) on density, compressive mechanical properties, and morphology of the material was reported, and the incorporation of 1.5 wt.% wood flour in phenolic foams led to a reinforced material with a compressive modulus and strength 130% and 154% of the values of the unreinforced foam, respectively (Del Saz-Orozco *et al*. 2014). The effects of azodicarbonamide (AZD) and nanoclay (NC) content on the foaming properties of HDPE/wheat straw flour (WSF) composites showed that the addition of AZD and NC had a negative effect on the foamed composites' impact resistance (Babaei *et al*. 2014).

Interfacial toughness and toughening mechanisms of a sandwich beam, consisting of aluminum foam covered with two carbon-fiber/epoxy composite surface layers, were investigated (Sun *et al*. 2012, 2013). The interfacial bonding was determined between the aluminum-foam core and carbon-fiber face sheets with short aramid fibers of different lengths and densities inserted at the face-core interface during the sandwich fabrication process. It was found that the short aramid fiber affected the structural performance effects on the structures. In the manufacture of the aluminum foam sandwich by a modified powder compact melting process it was found that the foaming process can be divided into three stages: pore forming, pore growing, and pore cracking. The microstructure evolved into a dendritic structure and eutectic phase (Wang *et al*. 2015).

In this work, the manufacture of lightweight sandwich engineered wood using eucalyptus fiber and epoxy adhesive wood foam as core was studied. The ultimate aim for

this lightweight material is reduction in the weight of construction panels. Three types of foaming agents**:** (*i*) thermal degradation, (*ii*) thermal/physical phase transformation, and (*iii*) physical expansion, were examined and compared. The best candidate was obtained for the lightweight sandwich engineered wood manufacture during the single step hot compression molding process.

EXPERIMENTAL

Materials

The main materials for manufacturing the wood foam core and the lightweight sandwich structure engineered wood were of commercial grade and categorized into five components: (*i*) epoxy-based adhesive, (*ii*) eucalyptus fiber, (*iii*) foaming agents, (*iv*) fiberglass cloth, and (*v*) teak veneer. The in-house prepreg-type polycarbonate (PC) blended epoxy was employed as a wood adhesive and also as the matrix for the fiberglass cloth reinforcement (Meekum and Wangkheeree 2017).

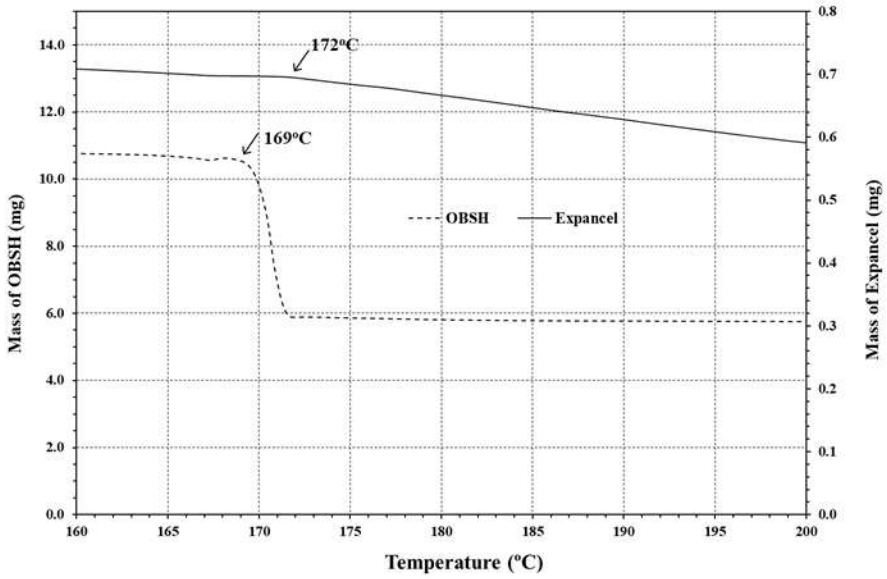

Fig. 1. TGA thermograms of OBHS and Expancel®

The eucalyptus fiber was available from Agro Fiber Co. Ltd., Prachinburi, Thailand. It was pre-vacuum dried at 105 °C for at least 4 h before use. The foaming agents employed were categorized, due to the formation of foam cell, into three types: solely thermal, thermal/physical, and solely physical induction. The 4,4' oxybis(benzene sulfonyl hydrazide) (OBSH) from A. F. Goodrich Chemicals Co., Ltd., Bangkok, Thailand was classified as the thermal agent. The foam cell was formed by the degraded gas at temperatures above 150 °C. Ethyl acetate (EA) was purchased from Ajax Finechem Pty Ltd. (Bangkok, Thailand). The cell was caused by physical transformation of liquid into gas vapor by heating above its boiling point, 77 °C. Expancel® Microsphere is an acrylic copolymer bead encapsulated with low-boiling blowing agents: isooctane and isobutane. It foamed by physical expansion when the bead was softened at temperatures above 125 °C.

It was kindly supplied from KEM KOTE Co., Ltd., Samutsakhon, Thailand. Figure 1 shows the TGA result OBSH and Expancel®.

It can be seen that the sharp decomposition temperature at 169 °C is evidenced for the OBSH. However, slowly decreasing in the weight loss, starting at 172 °C until 200 °C, is observed for the Expancel®. This reveals that the micro polymer bead begins to soften and expand due to the isooctane and isobutane expansion at 172 °C. If the full expansion of the bead is required, the heating temperature must be above 172 °C. In the observed tests, at least 180 °C was necessary. A comparison between OBSH and Expancel® as thermal induce foaming agents revealed that OBSH is more easily triggered by heating than Expancel®. Narrow processing temperature would be required for the OBSH, and v*ice versa*, a broader expansion temperature window is needed for the Expancel®.

Fiberglass cloth with the aerial density of 100 g/m^2 was used as the reinforcement for the manufacturing of lightweight sandwich structure engineered wood. It was laminated onto teak veneer skin faces. The fiberglass cloth was kindly provided from Cobra International Co., Ltd., Maung, Chonburi, Thailand. Teak veneer with 0.80-mm thickness was locally manufactured by slicing from the 25- to 30-year-old teak logs. The MDF, from Agro Fiber Co., Ltd., Prachinburi, Thailand, was used as a reference for the termite resistance testing.

Manufacturing of wood foam cores

Wood foam cores were manufactured *via* compression molding. A two-plate compression mold with a square cavity dimension (W × W × H) of 20 cm × 20 cm × 0.5 cm was employed. According to the calculated mold volume, 200 cm^3, the total weight of the eucalyptus fiber/epoxy adhesive was calculated in accordance with the assigned density. In this study, the adhesive content at 40 phr that corresponded to the fiber was employed. In the manufacturing process, the vacuum-dried eucalyptus fibers were vigorously beaten into pulp with a high-speed mixer chamber. The adhesive ingredients, including the assigned amount of foaming agent, were vigorously mixed. Approximately half of the mixed resin was immediately poured onto the pulpy fibers and robustly mixing for 30 s. Then, the remained epoxy was added and completely coated onto the fiber in the same fashion. The adhesive/foaming agent/fibers mixture was evenly transferred into the mold cavity pre-lined with poly(tetrafluoroethylene)(PTFE) sheets. The pre-forming was performed by cold compression at approximately 50 kg$_f$/cm^2 to 90 kg$_f$/cm^2 for a few minutes. Next, it was completely consolidated on the compression machine (GT-7014-A30, GoTech Testing Machine Inc, Taichung, Taiwan) at 180 °C and 120 kg$_f$/cm^2. The press (240 s)/decompress (5 s)/press (180 s) molding cycle was executed. The cured wood foam was demolded and annealed at room temperature overnight. The test specimens were saw-cut, edge-polished, and then post-cured at 120 °C for 12 h before testing.

Lightweight sandwich structure engineered woods

The 20 cm × 20 cm × 0.80 mm teak veneers were used as the skin faces of the lightweight sandwich structure engineered wood. They were reinforced with prepreg woven fiberglass, or GFRP, by a hand lay-up lamination. Two types of the sandwich structures were investigated: single (X1) and double layer (X2) of the wood foam core(s), according to the number of core, as shown in Fig. 2. The single step manufacturing process was adopted. All ingredients, including the calculated amount of fiber/adhesive/foaming agent and teak veneers reinforced with GFRP, were arrayed in the compression mold. Cold

and then hot compressions, with the identical condition as described in the production of the cores, were conducted. The test specimens were also obtained in the same fashion as previously explained (Meekum and Wangkheeree 2016). Both sandwich structures had the final thickness and density approx. of 5.0 mm and 0.75 g/cm^3, respectively.

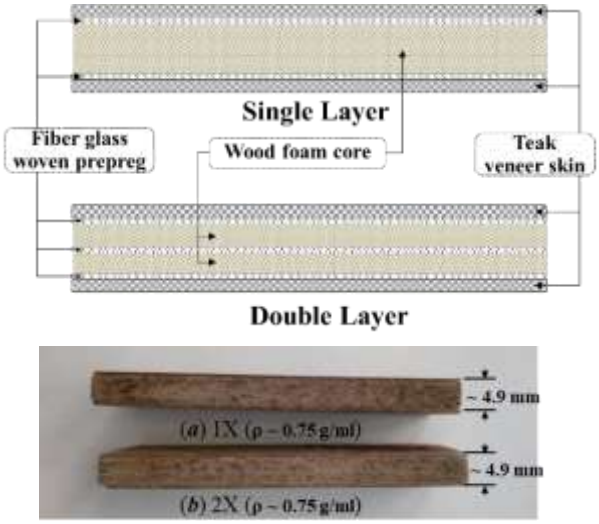

Fig. 2. Engineering drawing and photographs of the (**a**) single (X1) and (**b**) double (X2) layer of the lightweight sandwich structure engineered woods

Methods

Standard Testing

The mechanical properties were measured by means of three point bending fixture flexural, Izod impact strength, both notched and unnotched, in accordance with ASTM D790-10 (2010) and ASTM D256-10 (2010), respectively. The heat distortion temperature (HDT) was examined according to ASTM D648-07 (2007) at 1820 kPa loading. Durability evaluations based on water absorption (%, WA_i), thickness swelling (%, TS_i), and dimensional stability after removing a percentage of the moisture or thickness swelling after drying ($TS_{dried,i}$), after 1 day and 7 days of water immersion, were also performed in accordance with ASTM D570-98 (2010). The sample morphology was visually observed by a scanning electron microscope (SEM) with a JSM 6010LV, JEOL Ltd., Tokyo, Japan. The Mettler Toledo TGA/DSC1, Star System, Schwerzenbach, Switzerland was employed for measuring the decomposition temperature (T_d) of the foaming agents.

RESULTS AND DISCUSSION

Wood Foam Core Manufactured by OBSH Foaming Agent

Initially, there were two technical issues to be optimized: (*i*) OBSH concentration and (*ii*) density. First, at the 0.50 g/cm^3 designed density, the OBSH foaming agent was varied from 0 phr to 10 phr. Table 1 summarizes the tested properties of the 0.50 g/cm^3 cores, compression molded at 180 °C, and the OBSH contents. Notched and unnotched impact strengths showed the tendency to be fractionally increased when the OBSH content increased. However, exceeding 7 phr, the strengths, especially for the notched mode, were noticeably inferior. Similar trends were found for the flexural properties. The flexural

strength, modulus, and deformation at break clearly increased at the OBSH content from 4 phr to 10 phr. The marginal properties' improvement could have been explained by the internal compaction pressure effect. In the closed mold process, the larger presence of decomposed gas, the higher in internal pressure, or compaction force, and also the more foam cells. Consequently, at the given density, good foam cell, size distribution, and a denser foam shell wall would be obtained at a high OBSH content. Eventually, superior properties at high OBSH contents were witnessed. However, two issues must be taken into account: density and the fiber size. The unconsolidated bulk density of the eucalyptus fiber employed in this work was simply measured at approximately 0.0236 g/cm^3. The density of epoxy resin is typically around 1.10 g/cm^3 to 1.15 g/cm^3. Roughly speaking, the unconsolidated bulk density or critical minimum density ($\rho_{crit,min.}$) of the fiber coated with 40 phr of the epoxy adhesive would be in the range of 0.0330 g/cm^3 to 0.0334 g/cm^3 (Gibson 1994). This meant that the theoretical compression ratio, ($\rho_{wood}/\rho_{crit,min}$), applied for the wood foam manufacturing was approximately 15 times of critical minimum density of unconsolidated fiber. It was relatively low for the engineered wood compression process. For this reason, mechanical properties of the 0.50 g/cm^3 eucalyptus/epoxy wood foam were considerably weak. Evaluating the fiber size *via* the aspect ratio (L/d) was another justification. The higher that the aspect ratio of pulp fiber was, the lower the bulk density, and the larger amount of free volume. Such fiber would have a high compression ratio, at the given final density of the manufactured engineered wood. The eucalyptus fiber employed had an L/D ratio of approximately 50, as observed by SEM (Meekum and Wangkheeree 2016). It was a relatively low L/D ratio for natural fiber. Considering both the $\rho_{crit,min.}$ and the fiber size, this could have been why the properties of the 0.50 g/cm^3 manufactured wood foam using the OBSH as the foaming agent were quite weak. The statements were reinforced by the SEM photographs (30x) shown in Fig. 3 (a) through 3 (e), respectively. It was noticed that the loosely compacted wood fiber was generally seen at 0 phr to 4 phr of OBSH. But from 7 phr to 10 phr, the dense region of the fiber/epoxy adhesive was clearly seen. It confirmed that, without and at low OBSH content, a low compaction force between the fiber and adhesive was experienced. An increased amount of OBSH above 7 phr clearly formed the compacted area. The internal consolidated pressure, due to the degraded gas expansion, was the main phenomena. Hence, there was a stronger foam shell and superior mechanical properties of the resulting wood foam.

The WA_i, TS_i, and $TS_{dried,\ i}$, of the wood foam after 1 day and 7 days of water immersion, are reported in Table 2. As expected, the WA_i values showed the tendency to be lower, regardless of the soaking times, when the foaming agent increased. However, the thickness expansion, TS_i for 1 day, of the wood samples fractionally increased when OBSH increased from 0 phr to 4 phr, and v*ice versa*, at 7 phr and 10 phr, the TS_i exhibited a reverse trend. The TS_i was lowered as OBSH increased. However, with prolonged immersion for 7 days, the TS_i clearly decreased with the increased content of the OBSH foaming agent. The exact trend of the TS_i results was found for the $TS_{dried,\ I}$, at both 1 day and 7 days of testing. The durability results were in agreement with the justification explained in the previous mechanical properties and SEM analysis. At the assigned density, 0.50 g/cm^3, of wood foam, at 0 phr, without the foaming agent, and at 1 phr to 4 phr of OBSH, there was not enough degraded gas to form the internal compact pressure inside the closed mold. Therefore, the fiber/epoxy adhesive was cured with loose compaction. Consequently, water could have easily penetrated the wood foams, which resulted in high water absorption and the hydrostatic pressure expansion, thus a high TS_i value. A further

increase in the OBSH loading meant an upsurge in the amount of degraded gas. Then, the internal force would rise. Consequently, higher compacting pressure, highly dense fiber/adhesive must be obtained accordingly, that is not only superior in the wood foam structural properties but also with good water resistance. At this initial step, it could be visibly apparent that the properties of the 0.50 g/cm^3 wood foam manufactured using the OBSH foaming agent were fragile at loadings below 4 phr and that superior properties were established at above 7 phr loadings.

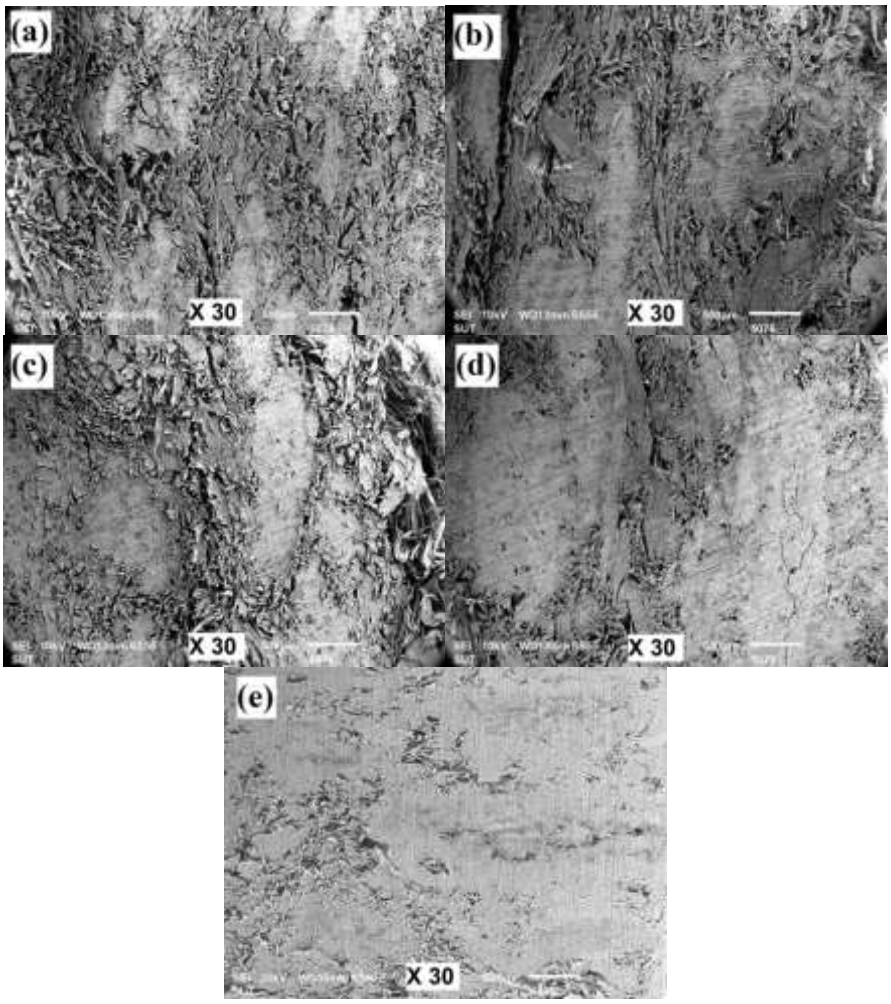

Fig. 3. SEM images of the wood foam core samples with final density of 0.50 g/cm^3 at (a) 0, (b) 1, (c) 4, (d) 7, and (e) 10 phr of OBSH (30x)

Table 1. Mechanical Properties of 0.5 g/cm^3 Wood Foams with OBSH Contents

Wood Foam	Density (g/cm^3)	OBSH (phr)	Impact Strengths (kJ/m^2)		Flexural Properties		
			Notched	Unnotched	Strength (MPa)	Modulus (GPa)	Max. Def.* (mm)
OBSH#1	0.50	0	1.85 ± 0.25	1.65 ± 0.42	3.07 ± 0.63	0.36 ± 0.06	2.85 ± 0.38
OBSH#2	0.50	1	2.00 ± 0.50	1.86 ± 0.42	2.37 ± 0.96	0.28 ± 0.14	2.35 ± 0.49
OBSH#3	0.50	4	2.77 ± 0.88	1.65 ± 0.45	2.20 ± 0.67	0.28 ± 0.16	2.25 ± 0.43
OBSH#4	0.50	7	2.24 ± 0.52	1.87 ± 0.33	3.12 ± 0.23	0.37 ± 0.05	3.67 ± 0.72
OBSH#5	0.50	10	1.55 ± 0.49	1.99 ± 0.49	4.39 ± 0.24	0.53 ± 0.04	3.05 ± 0.78

*Maximum deformation at beak

Table 2. Durability Test Results of Wood Foam Samples

OBSH (phr)	1 Day			7 Days		
	WA_i (%)	TS_i (%)	$TS_{dried,\ 1}$ (%)	WA_i (%)	TS_i (%)	$TS_{dried,\ i}$ (%)
0	116.5 ± 5.8	12.9 ± 0.3	2.1 ± 1.5	140.0 ± 16.5	15.6 ± 1.1	4.2 ± 1.2
1	104.7 ± 13.3	13.9 ± 4.0	1.8 ± 2.8	121.0 ± 7.9	15.5 ± 0.4	4.4 ± 0.6
4	123.8 ± 22.8	16.1 ± 1.0	3.8 ± 1.0	125.8 ± 10.8	15.1 ± 2.3	4.1 ± 1.0
7	100.9 ± 12.0	14.5 ± 1.8	2.5 ± 1.5	121.2 ± 12.2	14.2 ± 5.4	2.9 ± 4.7
10	116.2 ± 11.6	13.3 ± 0.7	2.2 ± 0.7	118.4 ± 13.3	13.9 ± 1.2	2.9 ± 1.1

Density Optimization of Wood Foam

Optimization of the wood foam core from 0.50 g/cm^3 to 0.90 g/cm^3 was explored. The specimens were produced using 10 phr of OBSH in the exact manner as described above. The measured properties *versus* density are summarized in Table 3. Undoubtedly, all of the tested properties, especially the mechanical ones, were clearly increased with increased density. For the HDT, only the density at 0.70 g/cm^3 to 0.90 g/cm^3 was able to be tested and showed that the service temperature was also gradually increased with the wood density. Below 0.60 g/cm^3, the samples were extremely loosely compacted. Therefore, they were unable to be tested because they could not withstand the calculated added weight at a 1820 kPa load. As manifested above, the properties relation of the final consolidated density of the wood foam was highly dependent on the compaction ratio, $\rho_{wood}/\rho_{crit,min}$. At a high compaction ratio producing the high-density wood, an excellently densified structure and good mechanical properties can be accomplished. Additionally, by introducing the internal consolidate pressure from the degraded gas expansion of the incorporated foaming agent, the densified fiber/adhesive would be heightened. Figures 4(a) through 4(e) demonstrate the SEM micrographs of the wood foam at density 0.50 g/cm^3 to 0.90 g/cm^3, manufactured from the epoxy adhesive and 10 phr OBSH foaming agent, respectively. The compaction of wood fiber/adhesive was clearly more aggregated with a greater density. The images confirmed the higher density *via* increasing the compaction ratio that led to more favorable properties.

Table 3. Properties of Wood Foam at Assigned Density Using OBSH

Wood Foam	Density (g/cm^3)	OBSH (phr)	Impact Strengths (kJ/m^2)		Flexural Properties			HDT (°C)
			Notched	Unnotched	Strength (MPa)	Modulus (GPa)	Max. Def. (mm)	
OBSH#0.5	0.50	10	1.55 ± 0.49	1.95 ± 0.40	4.39 ± 0.24	0.53 ± 0.04	3.05 ± 0.78	NA*
OBSH#0.6	0.60	10	2.25 ± 0.23	2.88 ± 0.68	9.42 ± 1.96	1.07 ± 0.14	2.65 ± 0.42	NA*
OBSH#0.7	0.70	10	2.69 ± 0.27	3.27 ± 0.26	11.08 ± 2.47	1.55 ± 0.22	2.15 ± 0.22	50.7 ± 1.5
OBSH#0.8	0.80	10	2.94 ± 0.27	4.30 ± 0.69	19.61 ± 1.54	2.31 ± 0.14	2.65 ± 0.29	54.2 ± 3.1
OBSH#0.9	0.90	10	3.27 ± 0.35	6.94 ± 0.61	33.20 ± 8.75	3.22 ± 0.59	3.03 ± 0.30	56.9 ± 2.5

*Samples were too loose to withstand the assigned standard load at 455 kPa

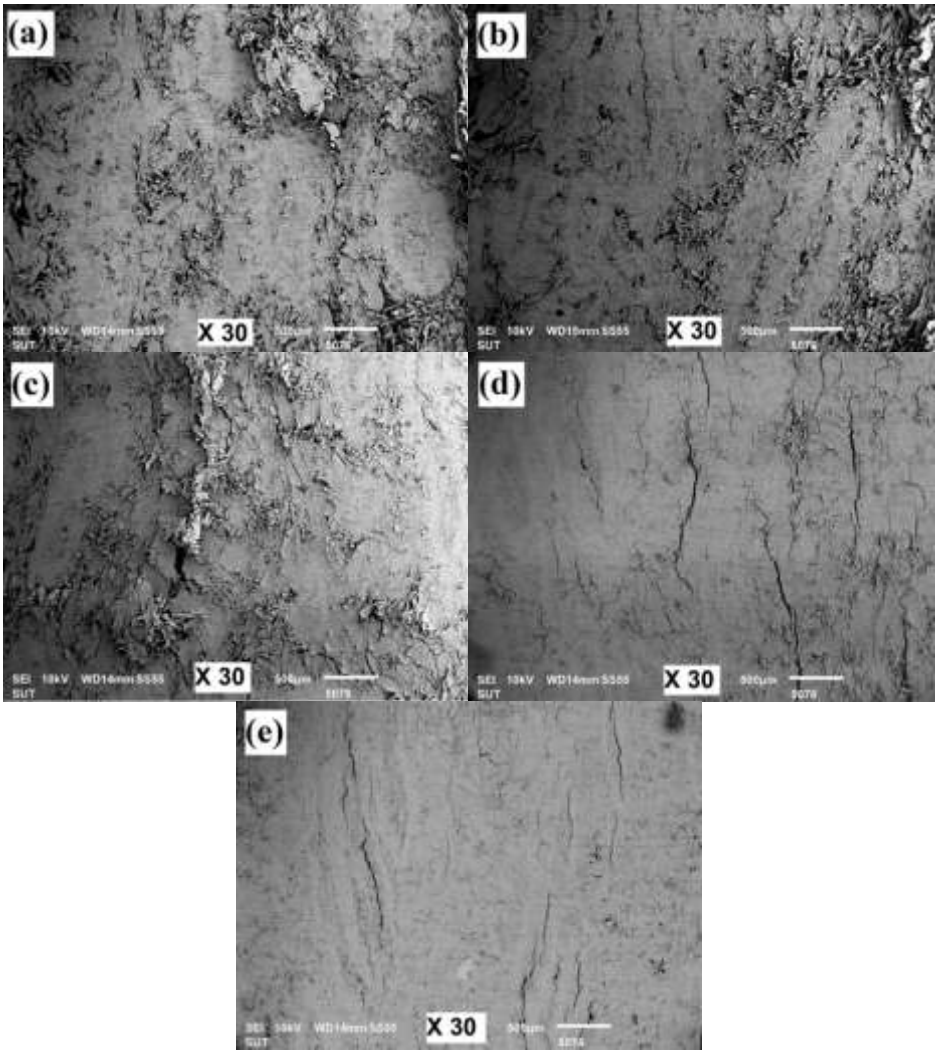

Fig. 4. SEM of (a) 0.50, (b) 0.60, (c) 0.70, (d) 0.80, and (e) 0.90 g/cm^3 of the wood foam (30x)

The resistance to the water absorption, as explained by the WA_i, TS_i, and $TS_{dried,\ i}$ of the wood foam is reported in Table 7. As expected, the percentage of WA_i, at both 1 day and 7 days were visibly decreased with increased density. For the TS_i, it had the tendency to be increased at a higher density. Similar to the $TS_{dried,\ i}$ at 1 day of immersion, it showed an increasing trend with density. However, at 7 days the results indicated a very low value with a high standard deviation of testing error. Nevertheless, no significant change in the $TS_{dried,\ i}$ at 7 days of immersion was evident. At a high compacted ratio, given the high wood density, highly densified fiber/adhesive would result. Hence, the water absorption, WA_i, into the structure must be lowered, and the higher the compaction force, the more stress residual on the fiber. Consequently, the thickness swelling, TS_i, of the wood due to the hydrostatic pressure must be increased at the higher density. Such as the domino effect, by removing the absorbed moisture *via* vacuum drying, the higher the residual stress at a high density, the higher the percentage of $TS_{dried,\ i}$. This statement was well explained by the percentage of $TS_{dried,\ i}$ at 1 day of immersion. For the 7 days of testing, the residual would be slowly relaxed upon prolonged immersion. Therefore, the final vacuum-dried thickness would not be changed.

Table 4. Durability Test Results of Wood Foam Derived Using OBSH foaming Agent with Density

Density (g/cm^3)	1 Day			7 Days		
	WA_i (%)	TS_i (%)	$TS_{dried,\ i}$ (%)	WA_i (%)	TS_i (%)	$TS_{dried,\ i}$ (%)
0.50	88.24 ± 3.63	13.13 ± 0.20	1.18 ± 0.20	73.40 ± 12.25	9.45 ± 0.86	1.07 ± 0.51
0.60	67.69 ± 3.35	13.66 ± 1.68	0.78 ± 0.89	81.34 ± 11.68	14.69 ± 1.72	0.91 ± 0.30
0.70	63.88 ± 16.26	16.84 ± 2.66	2.61 ± 1.83	67.89 ± 8.20	18.37 ± 0.79	1.09 ± 0.78
0.80	46.37 ± 10.16	17.28 ± 2.67	2.67 ± 1.36	62.13 ± 1.67	17.44 ± 0.82	0.57 ± 0.51
0.90	36.00 ± 11.03	16.11 ± 2.72	2.65 ± 1.98	44.55 ± 8.73	9.45 ± 0.86	1.09 ± 1.05

As mentioned, the achievement of a lightweight wood structure was the main goal for this research work. The wood foam core with low density but high mechanical properties is regarded as most desirable. Trading in-between density and performance properties at this stage, wood foam with the density of 0.70 g/cm^3 is preferable. Further research with using alternative foaming agents for manufacturing 0.70 g/cm^3 wood foam will be conducted in the future.

Wood Foam Core Manufactured From EA Foaming Agent

In this stage of the study, 0.70 g/cm^3 of wood foam were manufactured using the EA as the foaming agent. The contents varied from 10 phr to 20 phr. In the production, the assigned amount of EA was mixed with the epoxy adhesive and then incorporated with the fiber, because EA was represented as the thermal/physical foaming agent. Therefore, during the compression molding at 180 °C, the EA was heated and evaporated to form the foam cell inside the wood. The tested properties of the wood foam obtained *versus* the EA contents are illustrated in Table 5. According to the results obtained, it is apparent that all the mechanical means, impact strengths and flexural, were most likely to be enhanced by increasing the EA loading from 10 phr to 17 phr. When 20 phr was exceeded, the properties were lowered. Exactly the same trend was found for the HDT. The main factors to explain the correlation between the results obtained and the amount of EA used would be: (*i*) size, number and distribution of foam cell, (*ii*) form of foam cell (closed/opened), and (*iii*) shell strength of the foam cell. Generally, foam with the well-distributed small closed foam cells with high shell strength are preferable for the superior structural foam. In this study, 0.70 g/cm^3 of the wood foam produced in the fixed mold volume, at high EA content, meant a high volume of evaporated vapor gas. Also, it meant high internal consolidation pressure inside the mold cavity. Consequently, not only was the compaction force acting on the fiber/adhesive raised but also the number of foam cells with smaller sizes was increased. Therefore, the strengths of the wood foam structures were enhanced at high EA loadings. However, at the excessive EA dosing, *i.e.*, 20 phr, the extreme EA vapor gas volume would break and then collapse the closed cell structure of the wood foam. Accordingly, the performance properties of the foam would be terrible, as observed in this work. At 20 phr of EA, the wood foam became less ductile.

Figures 5(a) through 5(e) show the SEM photographs of the polished surface wood foam at the EA dosing from 10 phr to 20 phr, respectively.

Table 5. Properties of the Wood Foam Cores *versus* the EA Contents

Wood Foam	EA (phr)	Impact Strengths (kJ/m^2)		Flexural Properties			HDT (°C)
		Notched	Unnotched	Strength (MPa)	Modulus (GPa)	Max. Def. (mm)	
EA#1	10	3.22 ± 0.30	3.70 ± 0.47	10.00 ± 0.99	1.02 ± 0.12	3.50 ± 0.73	37.4 ± 0.72
EA#2	13	2.80 ± 0.25	3.41 ± 0.32	11.00 ± 1.06	1.08 ± 0.14	3.70 ± 0.54	38.5 ± 0.42
EA#3	15	3.14 ± 0.42	4.11 ± 0.66	12.56 ± 2.00	1.29 ± 0.18	3.05 ± 0.33	39.1 ± 0.81
EA#4	17	3.07 ± 0.31	4.13 ± 0.33	17.48 ± 1.38	1.46 ± 0.10	4.30 ± 0.62	38.6 ± 0.60
EA#5	20	3.14 ± 0.28	3.85 ± 0.29	13.00 ± 1.20	1.25 ± 0.07	3.20 ± 0.27	35.7 ± 0.95

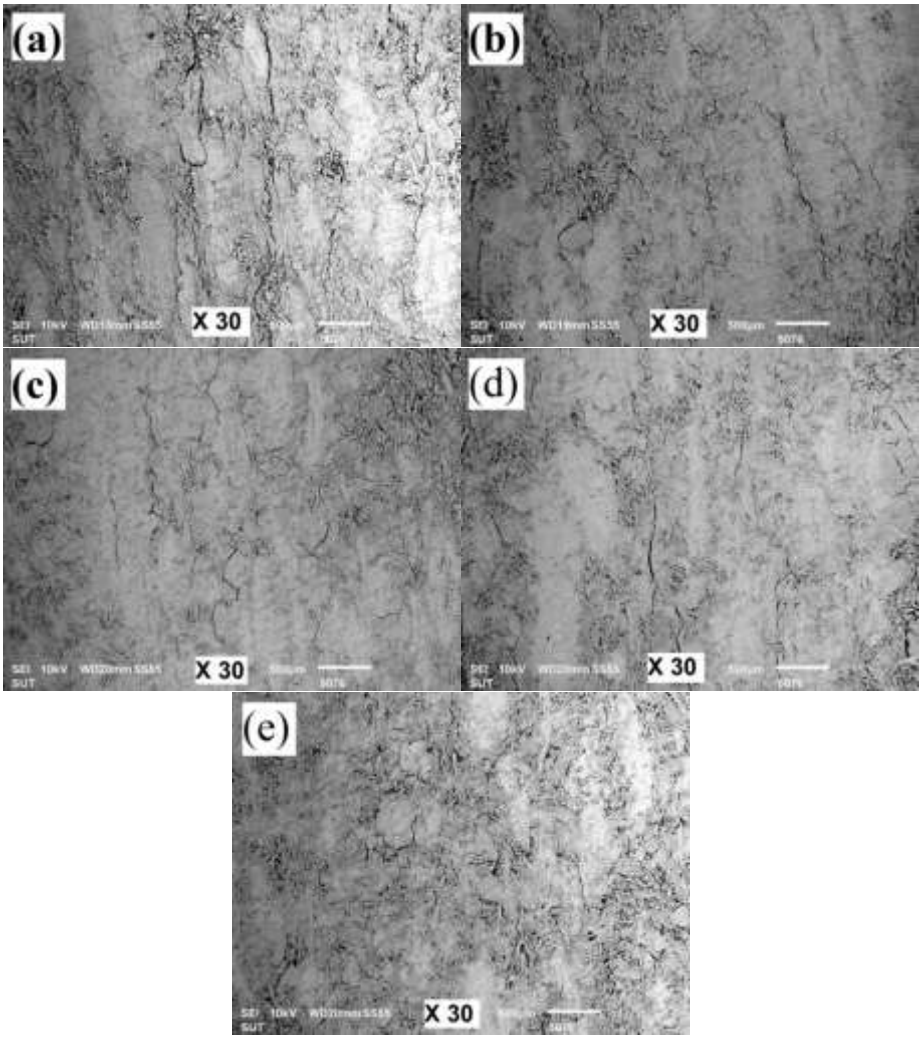

Fig. 5. SEM photographs of 0.70 g/cm^3 wood foam manufactured from (a) 10 phr, (b) 13 phr, (c) 15 phr, (d) 17 phr, and (e) 20 phr of EA loading (30x)

It was clearly apparent that the densification of fiber/adhesive was more intensified with increased EA loading. However, at 20 phr loading, it was clearly evidenced that the fiber/adhesive packing became looser. Thus, the SEM data reinforce the above hypothesized statements that a small closed-cell foam structure with good fiber/adhesive compaction would be achieved by increasing the EA foaming agent from 10 phr to

approximately 17 phr. Hence, the superior properties of the wood foam structure were gained. By exceeding the EA loading at 20 phr, an excessive vapor gas volume would occur. Moreover, a foam cell explosion would occur. In such cases, the foam cells would collapse. Consequently, the material's properties would be diminished.

The durability properties under water immersion for 1 day and 7 days were assessed. The WA_i, TS_i, and $TS_{dried,\ i}$, of the wood foam at the varied EA contents are inclusively reported in Table 6. The percent of WA_i, at both 1 day and 7 days immersion, slowly decreased as the EA content increased from 10 phr to 15 phr. At an excessive EA content above 15 phr, the percent of WA_i values showed a reverse trend. A similar trend was observed for the percent of TS_i and percent of $TS_{dried,\ i}$. It was noticeably decreased when the EA dose increased from 13 phr to 20 phr. There were two adsorption phenomena to be understood with this water resistivity testing: (*i*) closed and (*ii*) collapsed opened cells situations. In the closed cell foam structure, the water could be mainly absorbed into the fiber/adhesive foam shell. Therefore, with a high densified shell, a low WA_i value would have been perceived. According to this study, high densified foam cell was accomplished by increasing the EA dosing from 10 phr to 17 phr. Therefore, the WA_i was lower at higher EA contents. However, at above 17 phr loading, the collapsed opened cell structure was likely to occur. In the opened cell foam structure, more water could easily be absorbed into the broken cells. Hence, a high WA_i value must be expected. The closed and opened cell circumstances could be adopted to explain the thickness expansion of the wood foam before and after drying, respectively. On the closed cell samples a lower percent WA_i meant lower internal hydrostatic pressure. Hence, the percent of TS_i, and percent of $TS_{dried,\ i}$ were minimal. Nevertheless, on the broken opened cell wood foam structures with high percent of WA_i value, the water was absorbed into the inter-lamina plateau layers of the collapsed cell. The penetrated moisture would not have the effect on the increase in hydrostatic pressure as normally happens in the closed cell structure. For this reason, the percent of TS_i, and $TS_{dried,\ i}$. would not be changed with increasing the percentage of WA_i.

From the properties and EA dosage relationship of the 0.70 g/cm^3 wood foam, the mechanical properties were typically increased with an increase in EA content from 10 phr to 17 phr. The high densified fiber/epoxy adhesive foam shell structure that resulted from the rise in both internal pressure and volume of the vapor gas was considered. However, at an excessive amount of EA, 20 phr, the collapsing of the foam cell structure due to the explosive internal pressure of the vapor gas that caused inferior properties was in evidence. Taking the performance properties established in this section, the wood foam manufacture from 17 phr of EA was chosen as the best candidate for applying as the core in the lightweight sandwich engineered wood.

Table 6. Durability Test Results of 0.70 g/cm^3 Wood Foam with EA Loading

EA (phr)	1 Day			7 Day		
	WA_i (%)	TS_i (%)	$TS_{dried,\ i}$ (%)	WA_i (%)	TS_i (%)	$TS_{dried,\ i}$ (%)
10	90.19 ± 19.30	24.20 ± 1.44	9.00 ± 2.36	100.93 ± 9.24	25.19 ± 2.42	9.80 ± 2.51
13	86.08 ± 20.40	30.15 ± 4.74	12.71 ± 3.59	96.16 ± 9.88	27.61 ± 1.31	11.69 ± 0.50
15	76.89 ± 10.02	23.02 ± 1.74	6.59 ± 2.02	86.97 ± 9.05	24.78 ± 1.81	7.99 ± 2.13
17	81.64 ± 5.23	21.96 ± 0.81	6.02 ± 0.22	86.33 ± 3.19	22.83 ± 0.79	6.94 ± 0.99
20	92.85 ± 4.24	20.53 ± 1.59	5.70 ± 1.68	93.39 ± 4.95	21.89 ± 0.91	6.07 ± 0.19

Expancel® Microsphere as Foaming Agent

Expancel® is the trade name of acrylic copolymer micro-bead. It is encapsulated with low boiling point blowing agents: isooctane and isobutene. The bead is warmed to soften and then expanded at a temperature approximating 172 °C to 204 °C. Figure 6 shows the SEM picture of the Expancel® microsphere before and after placement in the closed mold at 180 °C for 8 min. It was seen that the bead was thermally expanded from an average diameter of 47 μm to 169 μm, which implies an expansion ratio of approximately 3.5 times. Beautifully uniform expanded closed cell foam was obtained from the microsphere bead. Various contents of the expandable microsphere were used to manufacture the wood foam with compression mold temperature at 180 °C in this study.

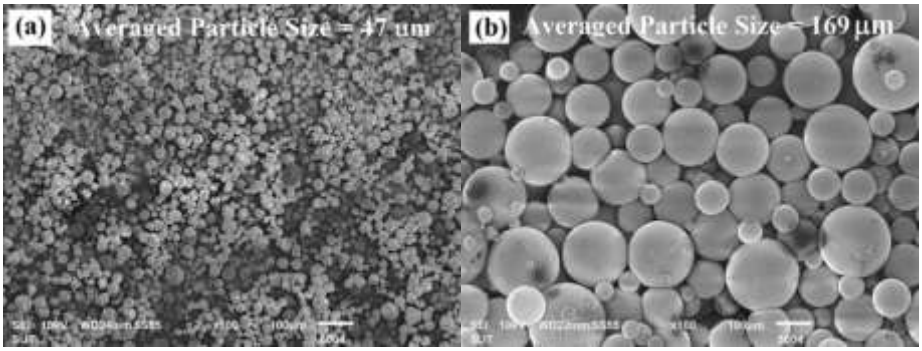

Fig. 6. SEM photographs of the Expancel®; (a) before and (b) after heating in the closed mold at 180 °C for 8 min (100x)

Table 7 summarizes the test outcome of 0.70 g/cm^3 wood foam with the Expancel® contents from 3 phr to 9 phr. Regarding the test outcome, the impact strengths, both notched and unnotched modes, seemed to have no remarkable change within the experimented microspheres loading. Similar trends of the results were also observed for the flexural properties. The HDT value, again, more or less did not depend on the microspheres content. Within the standard deviation of error, the HDT at 1820 kPa tested values were almost constant at approximately 35 °C.

An unexpected experimental outcome for the addition of the Expancel® foaming agent in the manufacturing of wood foam could be clarified by the SEM investigation. The SEM photographs of the sand-paper polished surface of the notched impacted specimen manufactured using Expancel® as the foaming agent at the content from 3 phr to 9 phr are presented in Figs. 7 (a) through 7 (d), respectively. It must be reminded that the mean diameter of the fully expanded microsphere foam cell was 160 μm, as evidenced in Fig. 5. With the "image scale" on the SEM photograph, the 160 μm traces of either the fully expanded or the pulled-out hole would be clearly seen on the surface of the investigated foam samples. According to the SEM results revealed in Fig. 6, there was no clear evidence of the expanded microsphere foam cell on the wood foam surface. Only small rounded particles with an approximate diameter of 50 μm were blurrily visualized by the SEM investigation. These particles were likely to be the unexpanded microsphere beads. This piece of evidence implied that the added expandable polymer microsphere was not thermally expanded under the given compression molding process conditions. One of the possible reasons that the microsphere polymer was not softened and then expanded into the foam cell could be the heat shielding effect from the fiber/adhesive mixture.

Table 7. Properties of Wood Foam Produced Using Expancel® Microsphere

Wood Foam	Density (g/cm³)	Expancel® Bead (phr)	Impact Strengths (kJ/m²)		Flexural Properties			HDT (°C)
			Notched	Unnotched	Strength (MPa)	Modulus (GPa)	Max. Def. (mm)	
Ex#1	0.70	3	2.86 ± 0.27	3.45 ± 0.29	14.82 ± 1.85	1.17 ± 0.12	4.88 ± 0.43	35.9 ± 1.1
Ex#2	0.70	5	2.98 ± 0.16	3.38 ± 0.20	12.63 ± 2.35	0.91 ± 0.11	6.06 ± 1.16	34.8 ± 0.6
Ex#3	0.70	7	2.65 ± 0.15	3.62 ± 0.29	14.92 ± 0.97	1.30 ± 0.02	3.88 ± 0.60	36.3 ± 1.0
Ex#4	0.70	9	2.72 ± 0.14	3.26 ± 0.20	14.70 ± 1.15	1.09 ± 0.06	5.05 ± 0.24	35.7 ± 1.1

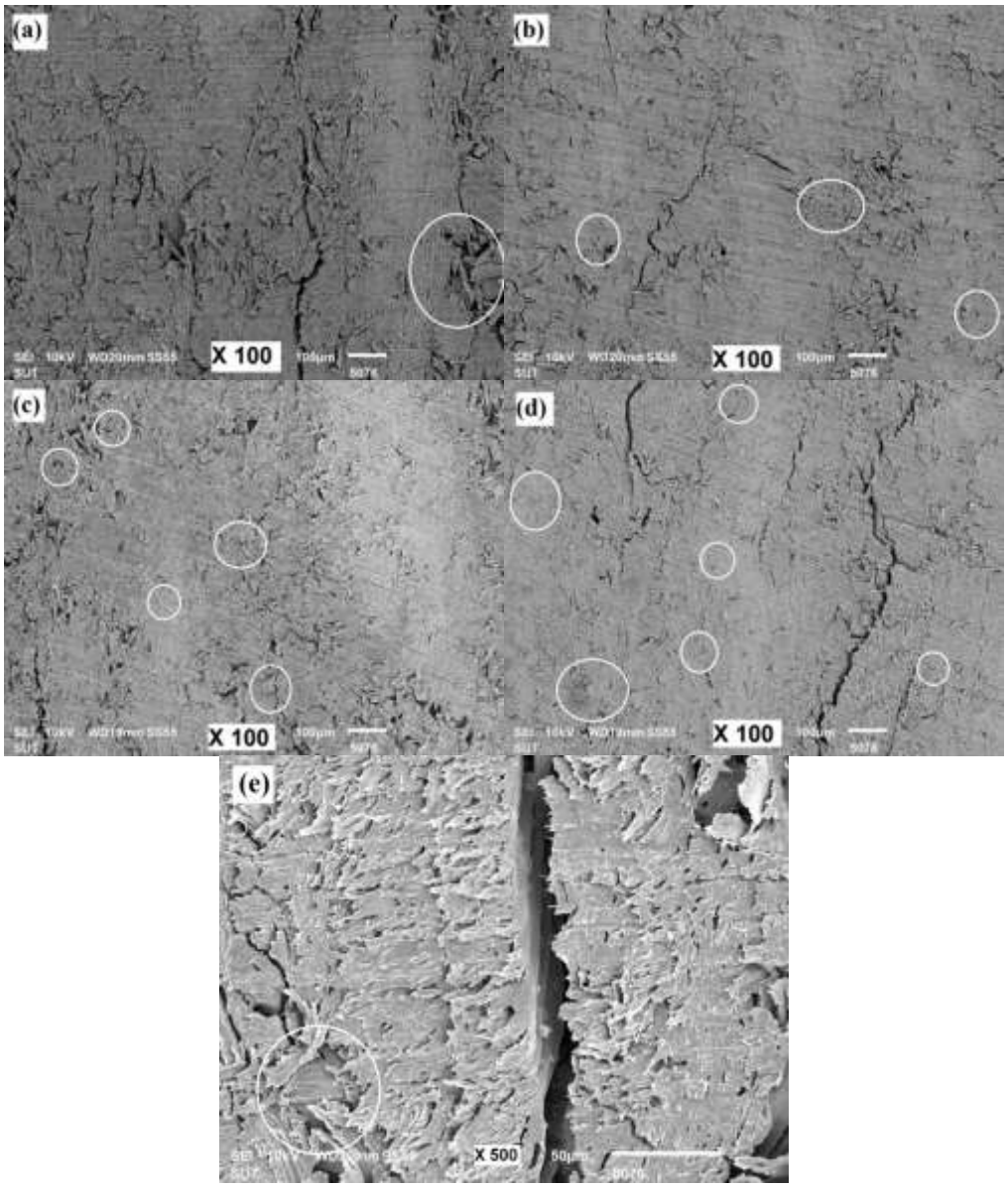

Fig. 7. SEM photos of 0.70 g/cm³ wood foam manufactured using (a) 3 phr, (b) 5 phr, (c) 7 phr, and (d) 9 phr of Expancel® foaming agent**,** at 100x and (e) 3 phr at 500x, respectively

As stated above and also evidence from the TGA result, the recommended expansion temperature for this microsphere is 172 °C to 204 °C. With the assigned

compression mold temperature at 180 °C, together with the heat shielding effect of the fiber/adhesive mixture, it would be insufficient to soften and expand the polymer bead. Further increasing the mold temperature beyond 180 °C would initiate the thermal degradation on fiber, which was the main ingredient for the foam product. Therefore, raising the mold temperature was not attempted.

The WA_i, TS_i, and $TS_{dried,\ i}$ measurements under water immersion of the Expancel® wood foam are reported in Table 8. The analyses revealed that the WA_i, TS_i and $TS_{dried,\ i}$, at both 1 day and 7 days of immersion, were marginally decreased with increasing the expandable microspheres content from 3 phr to 9 phr, respectively. The less than superior durability properties of the wood foam *via* increasing the Expancel® loading could have been explained by the hydrophobicity of the polymer bead and density fluctuation. It is well-known that the expandable microsphere, which is the acrylic polymer, is hydrophobic in nature. Therefore, the more microsphere that was added, the less water absorption that occurred. Another likely explanation came from the fact that increasing a small amount of the microsphere bead into the fiber/adhesive mixture meant increasing the weight/volume ratio on the molding. As a result, the obtained foam density was greater and the fiber/adhesive was more densified, at high bead loadings. For that reason, less water infusion and low thickness expansion of the densified wood foam would be achieved.

Table 8. Durability Test results of 0.70 g/cm^3 Wood Foam Made from Expancel® Foaming Agent

Expancel® (phr)	1 Day			7 Day		
	WA_i (%)	TS_i (%)	$TS_{dried,\ i}$ (%)	WA_i (%)	TS_i (%)	$TS_{dried,\ i}$ (%)
3	73.67 ± 3.61	21.50 ± 2.43	5.43 ± 1.21	83.89 ±	18.22 ±	4.02 ± 1.76
5	64.25 ± 2.43	17.81 ± 1.00	2.73 ± 0.96	76.45 ± 6.83	17.75 ±	3.49 ± 0.38
7	62.10 ± 0.47	16.39 ± 0.81	2.55 ± 2.79	69.86 ± 2.08	16.27 ±	2.71 ± 1.45
9	58.43 ± 3.67	16.34 ± 0.26	2.35 ± 0.10	64.56 ± 1.91	16.73 ±	2.50 ± 0.77

Manufacturing of Lightweight Sandwich Structure Engineered Woods

The above conclusion shows the optimal content of the three types of foaming agent; (*i*) the thermal degradation, OBHS, (*ii*) thermal/physical, EA, and (*iii*) physical, Expancel®, foaming agents used for the production of 0.70 g/cm^3 wood foam cores. The OBSH, EA, and Expancel® at 10 phr, 17 phr, and 7 phr, with respect to the fiber, were preferable contents, respectively. Those formulations were adopted for manufacturing the core material and applied in the production process of the lightweight sandwich structures engineered wood in a single step production. Two types of sandwich structures were investigated in this work: single (X1) and double (X2) layer(s), as shown in Fig. 1. The fiberglass woven prepreg in conjunction with teak veneer were employed as skins of the lightweight sandwich structures. They also acted as the structural reinforcement. One of the main industrial applicable objectives for the lightweight sandwich structure engineered wood reinforced with fiberglass woven was the decorative/structural panel part of the residential building. Then, the teak veneer performed not only as the aesthetic part but also as the mechanical strength of the panel. The tested properties of the lightweight sandwich structures, obtained from the above optimal wood foam core formula, are summarized in Table 9.

Table 9. Properties of the Lightweight Sandwich Structure Derived from Different Wood Foam Cores

Woods	Foaming Agent	Content (phr)	Impact Strength(kJ/m^2)	
			Notched	Unnotched
Core	OBSH	10	2.69 ± 0.27	3.27 ± 0.26
X1			16.47 ± 1.91	25.17 ± 1.97
X2			19.13 ± 1.21	32.26 ± 1.90
Core	EA	17	3.07 ± 0.31	4.13 ± 0.33
X1			20.69 ± 0.38	26.13 ± 1.20
X2			19.38 ± 0.20	30.82 ± 2.98
Core	Expancel®	7	2.66 ± 0.20	3.65 ± 0.47
X1			18.91 ± 1.17	23.74 ± 1.77
X2			20.10 ± 0.94	26.82 ± 2.49

Woods	Foaming Agent	Content (phr)	Flexural Properties			HDT (°C)
			Strength (MPa)	Modulus (GPa)	Max. Def. (mm)	
Core	OBSH	10	11.08 ± 2.47	1.55 ± 0.22	3.05 ± 0.78	50.7 ± 1.53
X1			74.78 ± 9.80	5.59 ± 1.24	2.89 ± 0.38	116.5 ± 6.82
X2			111.83 ± 7.09	5.62 ± 1.19	3.56 ± 0.25	118.3 ± 4.02
Core	EA	17	17.48 ± 1.38	1.46 ± 0.10	4.30 ± 0.62	38.6 ± 0.60
X1			60.70 ± 4.07	3.48 ± 0.95	2.73 ± 0.16	74.1 ± 7.37
X2			56.73 ± 3.19	4.35 ± 0.63	2.71 ± 0.28	77.1 ± 9.87
Core	Expancel®	7	14.54 ± 2.06	1.26 ± 0.12	3.94 ± 0.55	36.3 ± 0.99
X1			67.32 ± 9.97	3.14 ± 1.14	3.23 ± 0.54	95.9 ± 8.45
X2			74.75 ± 6.12	3.76 ± 0.66	3.78 ± 0.28	98.5 ± 4.80

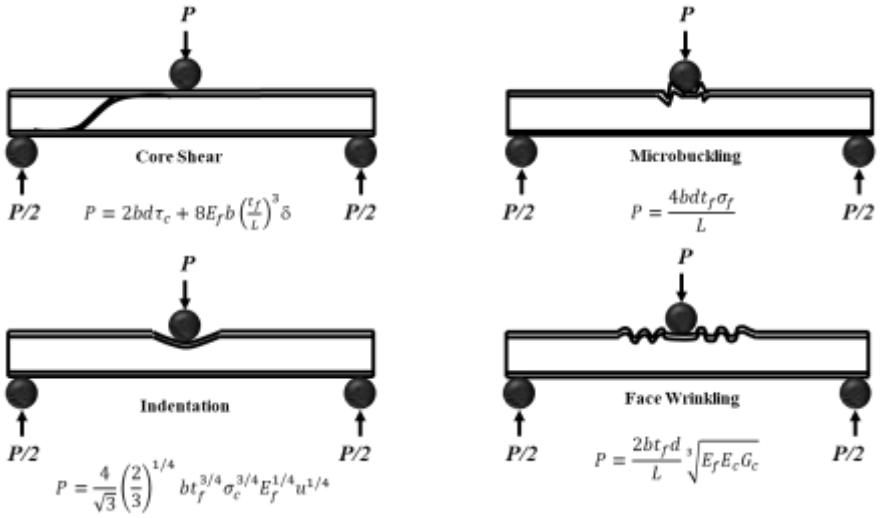

(*a*)

Fig. 8a. Failure modes of a sandwich beam in three-point bending of the lightweight wood foam core sandwich structures

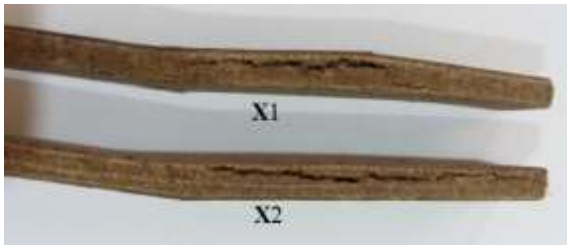

(*b*)

Fig. 8b. Failure modes of a sandwich beam in core shear failure of X1 and X2 the lightweight wood foam core sandwich structures

Generally, there are four mode of the sandwich collapse when subjected to the three-point and four-point bending; (*i*) core shear, (*ii*) micro buckling, (*iii*) Indentation, and (*iv*) face wrinkling as shown in Fig. 8(a) (Craig and Norman 2004). For a sandwich beam in three-point bending, the collapse loads (*P*) are predicted by the following equations;

$$\text{Core shear} \qquad P = 2\tau_c bd \tag{1}$$

$$\text{Microbuckling} \qquad P = \frac{4\sigma_f b t_f d}{L} \tag{2}$$

$$\text{Indentation} \qquad P = b t_f \left(\frac{\pi^2 \sigma_c^2 E_f d}{3L}\right)^{1/3} \tag{3}$$

$$\text{and} \quad \text{Face wrinkling} \qquad P = \frac{2 b t_f d}{L} \sqrt[3]{E_f E_c G_c} \tag{4}$$

where L = span length, b = beam width, d = core thickness, t_f = face thickness, E = Young's modulus, G_c = shear modulus, σ_c = compressive strength, and τ_c = shear strength, respectively. In this work, only "*core shear*" failure mode was clearly observed, as seen in Fig. 8(*b*), on the lightweight sandwich structure manufactured from the wood foam cores. Therefore, Eq. (1), the core shear collapse load prediction, would be obeyed. With identical face material performance and specimen dimension, the failure load (*P*) of the obtained sandwich is mainly dependent on just the shear strength of the core(τ_c). This means that the greater the core shear strength the greater will be the failure load of the sandwich structure. In the X2 structure, a layer of prepreg GFRP was inserted at the middle of the wood foam core. The higher shear strength of the core was expected. Therefore, higher failure load, comparing to the X1 structure, would result.

According to the measured values and together with the above predicted equation, the results can be interpreted. At the given wood foam core material, it was clearly evidenced that all mechanical and thermal, HDT, and properties of the sandwich structure were much higher than those of its core. As expected, it was also seen that the X2 structure was superior to that of the X1 structure. During the flexural measurement, only the "core shear" failure mode was observed. There was absolutely no delamination involving the faces. This indicated excellent inter-lamina bonding between the core and teak/glass skins. However, in comparison between the impact and flexural tests, in the "Izod mode" of impact testing, the force was acted on in the edgewise direction perpendicular to the laminated layers of the sample. The impact energy is the energy required to break apart of the test specimen. In case of the sandwich specimen obtained in this study, the Teak/GFRP skins are the strongest constituent. Therefore, most of the impact energy is used to break the skins. Therefore, the impact strength was dominantly dependent on the skin materials,

not on the core one. As a result, there was not much difference in the impact strengths between the X1 and X2 structures. In addition, on the three point bending flexural test, failure of the specimen was induced by the flatwise, machine direction, loading force. Obeying the "core shear" failure mode, the flexural strength is largely dependent on the core performance. With good lamination adhesion, the X2 sandwich structure showed more enhancement than the X1 structure, regardless of the type of wood foam core used in this study.

Among the three types of wood foam core manufactured from those three foaming agents, the core made from EA showed the most favorable mechanical properties. The OBSH foam came in second with a small margin. However, when the EA foam was applied into the lightweight sandwich structure, the structures derived from the EA wood foam core, both X1 and X2, did not always manifest the mechanical superiority among those three structures. Generally, the lightweight sandwich engineered woods, both X1 and X2, made from the OBSH foaming agent showed more advancement in the mechanical and HDT properties, especially under the bending flexural test, compared to the other two. As theoretically mentioned above, it can be stated that the outstanding mechanical properties of the lightweight sandwich structure made from the wood foam cores and teak veneer reinforced with prepreg GFRP skins were certainly contributed mainly from the core.

By submersion of the wood foam cores and X1 and X2 lightweight sandwich engineered woods produced, using three types of foam agents, in water for 1 day and 7 days the WA_i, TS_i, and $TS_{dried,\ i}$, results are illustrated in Table 10. The WA_i values at both 1 day and 7 days of immersion were noticeably decreased from the core to the X2 structures, regardless of the type of core material. The trend indicated good water resistance. Also, it was revealed that the teak/CFRP skins acted as protective layers to prevent water penetration at the surfaces of the wood foam core. When the three foam cores were compared, the wood foam produced by OBSH showed the lowest WA_i. The EA gave rise to the worst water resistance with the highest WA_i value. The trend was adopted when applying those cores for making the X1 and X2 lightweight sandwich engineered wood. For the TS_i, a trend similar to the WA_i results was observed. The core derived from the EA foaming agent showed the highest TS_i. In the case of the $TS_{dried,\ i}$ test values, the highest $TS_{dried,\ i}$ was seen on the EA wood. In a comparison between X1 and X2 structures at identical sample thickness, the thickness stability enhancement, a low $TS_{dried,\ i}$ value was evidenced, irrespective to the type of cores. The lightweight sandwich structures manufactured from the other cores also manifested the similar tendency. Obeying the obtained durability testing, WA_i, TS_i, and $TS_{dried,\ i}$, the ability to absorb water of the lightweight sandwich engineered wood was mainly dependent on the characteristic of the core material. By introducing the teak/GFRP skins to the sandwich structure they also acted as the protective layers from the surficial water absorption.

The X1 and X2 layers of lightweight sandwich structure engineered wood from the teak/CFRP skins and wood foam cored using different foaming agents was manufactured with effective inter-lamina bonding. The properties' enhancement of the sandwich structures was mainly contributed from the skins materials. In the development of X1 and X2, with the same volume fraction of core, the marginal increase in the properties due to the contribution of the added thin interlaminated GFRP layer was observed. The contribution of the core properties on the final performance of the sandwich structures was also noticed. The structures made from 10 phr OBSH foaming agent core seemed to have the most superior properties.

Table 10. Durability Test Results of Lightweight Sandwich Structures Made from Three Different Wood Foam Cores

Woods	Foaming Agent	Content (phr)	1 Day		
			WA_i (%)	TS_i (%)	$TS_{dried,\ i}$ (%)
Core	OBSH	10	63.88 ± 16.26	16.84 ± 2.66	2.61 ± 1.83
X1			62.29 ± 8.79	11.74 ± 0.63	1.42 ± 0.54
X2			44.56 ± 4.88	13.23 ± 0.49	1.49 ± 0.49
Core	EA	17	81.64 ± 5.23	21.96 ± 0.81	6.02 ± 0.22
X1			70.88 ± 2.83	15.62 ± 0.90	5.59 ± 0.49
X2			66.90 ± 4.77	18.85 ± 0.29	4.95 ± 1.11
Core	Expancel®	7	62.10 ± 0.47	16.39 ± 0.81	2.55 ± 2.79
X1			59.44 ± 0.94	9.51 ± 0.42	2.09 ± 0.42
X2			52.95 ± 3.24	12.03 ± 0.30	2.46 ± 0.74

Woods	Foaming Agent	Content (phr)	7 Days		
			WA_i (%)	TS_i (%)	$TS_{dried,\ i}$ (%)
Core	OBSH	10	67.89 ± 8.20	18.37 ± 0.79	1.09 ± 0.78
X1			60.60 ± 10.90	12.46 ± 1.14	0.34 ± 0.78
X2			44.25 ± 4.89	13.73 ± 0.28	0.27 ± 0.24
Core	EA	17	86.33 ± 3.19	22.83 ± 0.79	6.94 ± 0.99
X1			69.02 ± 3.41	16.74 ± 1.22	5.42 ± 0.25
X2			68.10 ± 2.56	17.98 ± 1.43	2.61 ± 0.47
Core	Expancel®	7	69.86 ± 2.08	16.27 ± 2.63	2.71 ± 1.45
X1			61.22 ± 4.68	13.04 ± 1.70	1.54 ± 0.30
X2			54.25 ± 4.71	13.15 ± 1.65	2.11 ± 0.82

Termite Resistance Evaluation

Figure 9 shows the wt.% *versus* buried time for the termite resistance testing of the woods. The wood samples were buried in a termite nest for 18 weeks. Teak, Para-rubber, and commercialized urea-based adhesive MDF, with an approximate density of 0.7 g/cm^3 to 0.8 g/cm^3, woods were used as references. Teak is known to be the most termite resistant wood.

Para-rubber is a soft wood and is less resistant to termite attack. According to the results, it was clearly seen that the commercialized MDF was completely consumed by the termites within 9 weeks, followed by the Para-rubber within 14 weeks. However, the teak and X2 lightweight sandwich were in good shape after burial in the termite net for more than 18 weeks.

Meanwhile, almost 80 wt.% of OBSH wood foam and X1 lightweight sandwich engineered wood were compact shaped after 18 weeks of burial. Only the edges of the specimen were attacked by the insect. This showed that the epoxy adhesive used on the teak/CFRP skins not only enhanced the physical properties of the man-made woods but also protected the wood material from the termite attack.

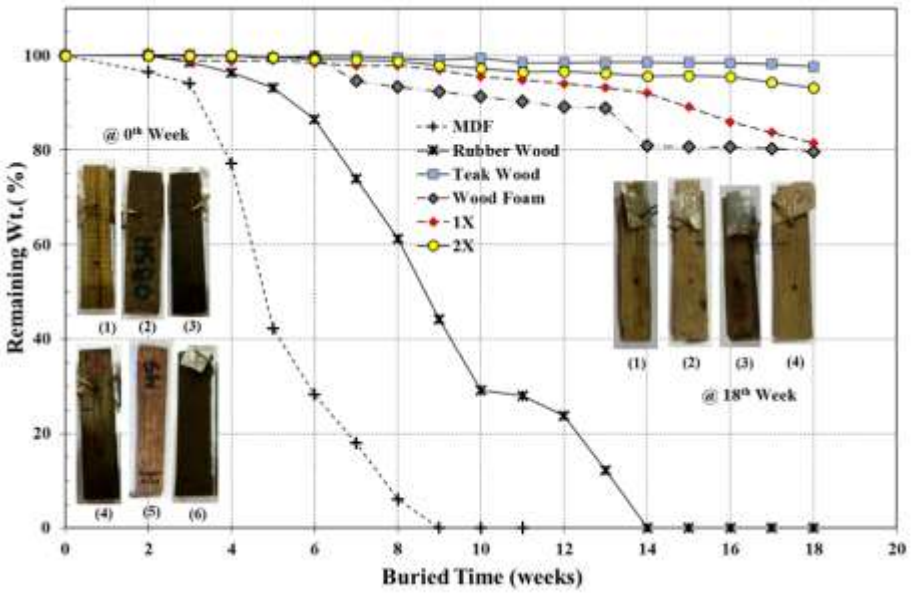

Fig. 9. The remaining wt.% *vs.* buried time for the termite testing: (1) Teak, (2) OBSH wood foam, (3) 1X, (4) 2X, (5) Para, and (4) MDF wood

CONCLUSIONS

1. For manufacturing the 0.50 g/cm^3 wood foam using the OBSH as a foaming agent, it was found that material had inferior properties when the foaming agent loading was less than 4 phr. It was noticed that superior properties were seen by increasing the OBSH loading into the epoxy adhesive. The increase in the amount of the degraded gas was associated with the properties improvement. The internal consolidated pressure from the degraded gas expansion generated the bubble foam cell and then compacted the fiber/adhesive to form the foam shell. An OBSH loading above 7 phr was recommended for superior properties of the wood foam.
2. The density optimization of the eucalyptus/epoxy adhesive wood foam using the OBSH foaming agent was at the loading content of 10 phr. The mechanical properties increased with increased wood foam density. The high-density fiber/epoxy adhesive structure due to high compaction ratio in the wood foam samples was important for the properties enhancement. Rationalization between the density and performance properties was obtained, and the wood foam at the density of 0.70 g/cm^3 was preferred and used as the desired density.
3. The EA was employed as an alternative foaming agent to manufacture the 0.70 g/cm^3 wood foam. It was found that the mechanical properties increased with increased EA content to approximately 15 phr to 17 phr. High densified fiber/epoxy adhesive foam shell structure due to the increase of internal pressure of the degraded vapor gas at high EA loading was postulated for the superior properties of the foam. Meanwhile, an excessive amount of EA at above 17 phr, collapsed the foam cell structure due to the explosive pressure of the evaporated gas and the properties insufficiency was observed. Thus, the 17 phr of EA content was highly recommended for manufacturing the wood foam core.

4. The use of expandable microsphere polymer bead or Expancel® as another alternative physical foaming agent was explored, and it was found that the incompetency properties of the wood foam were observed with the microsphere bead loading. The rationalization for the experimental outcome was explained by non-expansion of the polymeric microsphere. The bead was not able to expand to form the foam cell structure inside the wood core at 180 °C mold temperature for 8 min. Heat shielding by the fiber/adhesive mixture inside the compression mold was postulated. Consequently, insufficient heat conduction was experienced. Then, incomplete expansion of the microsphere foaming agent occurred.
5. In comparison among those three types of wood foam at the designed density of 0.70 g/cm^3, the EA core seemed to have marginally superior mechanical properties over OBSH, but the OBSH core showed outstanding durability characteristics. Meanwhile, using the expandable microsphere polymer as the foaming agent gave rise to the worst mechanical performance.
6. Applying the obtained wood foam cores into the manufacturing of X1 and X2 lightweight sandwich structure engineered woods with teak/GFRP as the skins resulted in good inter-laminar bonding. The "core shear" failure mode under the flexural bending was evidenced. The properties enhancement of the X1 and X2 sandwich structures was mainly contributed from core materials. At the same volume fraction of core, the marginal increase in the properties of X1 and X2 structures due to core enhancement by adding GFRP layer was observed. The contribution of the core properties on the final performance of the sandwich structures was also justified. The sandwich structure made from OBSH foam core had superior mechanical performance and HDT. Meanwhile, the lightweight sandwich wood made from the EA wood foam core was inadequate in terms of moisture/water absorption and thickness swelling.
7. The 0.70 g/cm^3 wood foam and its X1 and X2 lightweight sandwich structures manifested excellent resistance to the termite attack.

REFERENCES CITED

ASTM D256-10 (2010). "Standard test methods for determining the izod pendulum impact resistance of plastics," ASTM International, West Conshohocken, PA.

ASTM D570-98 (2010). "Standard test method for water absorption of plastics," ASTM International, West Conshohocken, PA.

ASTM D648-07 (2007). "Standard test method for deflection temperature of plastics under flexural load in the edgewise position (withdrawn 2016)," ASTM International, West Conshohocken, PA.

ASTM D790-10 (2010). "Standard test methods for flexural properties of unreinforced and reinforced plastics and electrical insulating materials," ASTM International, West Conshohocken, PA.

Babaei, I., Madanipour, M., Farsi, M., and Farajpoor, A. (2014). "Physical and mechanical properties of foamed HDPE/wheat straw flour/nanoclay hybrid composite," *Composites Part B- Engineering* 56, 163-170. DOI: 10.1016/j.compositesb.2013.08.039

Chand, N., Fahim, M., Sharma, P., and Bapat, M. N. (2012). "Influence of foaming agent on wear and mechanical properties of surface modified rice husk filled polyvinylchloride," *Wear* 278-279, 83-86. DOI: 10.1016/j.wear.2012.01.002

Chen, Y., Das, R., and Battley, M. (2015). "Effects of cell size and cell wall thickness variations on the stiffness of closed-cell foams," *International Journal of Solids and Structures* 52, 150-164. DOI: 10.1016/j.ijsolstr.2014.09.022

Craig, A. S. and Norman, A. P. (2004). "Collapse of sandwich beam with composite faces and a foam core, loaded in three-point bending. Part II: Experimental investigation and numerical modelling," *International. Journal of Mechanical Sciences* 46, 585-608. DOI: 10.1016/j.ijmecsci.2004.04.004

Del Saz-Orozco, B., Alonso, M. V., Oliet, M., Domínguez, J. K., and Rodriguez, F. (2014). "Effects of formulation variables on density, compressive mechanical properties and morphology of wood flour-reinforced phenolic foams," *Composites Part B- Engineering* 56, 546-552. DOI: 10.1016/j.compositesb.2013.08.078

Denes, L., Kovacs, Z., Elemer, M. L., and McGraw, B. (2008). "Investigation of the compression and bending strength of veneer-polyurethane foam composites," in*: The 51st International Convention of Society of Wood Science and Technology*, Concepción, Chile.

Dweib, M. A., Hu, B., O'Donnell, A., Shenton, H. W., and Wool, R. P. (2004). "All natural composite sandwich beams for structural applications," *Composite Structures* 63(2), 147-157. DOI: 10.1016/S0263-8223(03)00143-0

Fajrin, J., Zhuge, Y., Bullen, F., and Wang, H. (2013). "Significance analysis of flexural behaviour of hybrid sandwich panels," *Open Journal of Civil Engineering* 3*(*3B*)*, 1-7. DOI: 10.4236/ojce.2013.33B001

Fang, H., Sun, H., Liu, W., Wang, L., Bai, Y., and Hui, D. (2015). "Mechanical performance of innovative GFRP-bamboo-wood sandwich beams: Experimental and modelling investigation," *Composites Part B- Engineering* 79, 182-196. DOI: 10.1016/j.compositesb.2015.04.035

Gibson, R. F. (1994). *Principles of Composite Material Mechanics*, McGraw-Hill, Inc., Singapore.

Kedar, S. P., Veerraju, C., and Naik, N. K. (2011). "Hybrid composites made of carbon and glass woven fabrics under quasi-static loading," *Materials and Design* 32*(7)*, 4094-4099. DOI: 10.1016/j.matdes.2011.03.003

Mazzon, E., Habas-Ulloa, A., and Habas, J. -P. (2015). "Lightweight rigid foams from highly reactive epoxy resins derived from vegetable oil for automotive applications," *European Polymer Journal* 68, 546-557. DOI: 10.1016/j.eurpolymj.2015.03.064

Meekum, U., and Wangkheeree, W. (2016). "Manufacturing of lightweight sandwich structure engineered wood reinforced with fiberglass: Selection of core materials using hybridized natural/engineered fibers," *BioResources* 11*(*3*)*, 7608-7623. DOI: 10.15376/biores.11.3.7608-7623

Meekum, U., and Wangkheeree, W. (2017). "Designing the Epoxy Adhesive Formulation for Manufacturing Engineered Wood," *BioResources* 12*(2)*, 3351-3370. DOI: 10.15376/biores.12.2.3351-3370

Mohamed, M., Anandan, S., Huo, Z., Birman, V., Volz, J., and Chandrashekhara, K. (2015). "Manufacturing and characterization of polyurethane based sandwich composite structures," *Composite Structures* 123, 169-179. DOI: 10.1016/j.compstruct.2014.12.042

Pishan, S., Ghofrani, M., and Kermanian, H. (2014). "Study on mechanical properties of lightweight panels made of honeycomb and polyurethane cores," *Lignocellulose* 3, 59-68.

Poapongsakorn, P., and Carlsson, L. A. (2013). "Fracture toughness of closed-cell PVC foam: Effects of loading configuration and cell size," *Composite Structures* 102, 1-8. DOI: 10.1016/j.compstruct.2013.02.023

Soares, F. A., and Nachtigall, S. M. B. (2013). "Effect of chemical and physical foaming additives on the properties of PP/wood flour composites," *Polymer Testing* 32(4), 640-646. DOI: 10.1016/j.polymertesting.2013.02.009

Sun, Z., Hu, X., Sun, S., and Chen, H. (2013). "Energy-absorption enhancement in carbon-fiber aluminum-foam sandwich structures from short aramid-fiber interfacial reinforcement," *Composites Science and Technology* 77, 14-21. DOI: 10.1016/j.compscitech.2013.01.016

Sun, Z., Jeyaraman, J., Sun, S., Hu, X., and Chen, H. (2012). "Carbon-fiber aluminum-foam sandwich with short aramid-fiber interfacial toughening," *Composites Part A: Applied Science and Manufacturing* 43*(*11), 2059-2064. DOI: 10.1016/j.compositesa.2012.06.002

Vaikhanski, L., and Nutt, S. R. (2003). "Fiber-reinforced composite foam from expandable PVC microspheres," *Composites Part A- Applied Science and Manufacturing* 34(12), 1245-1253. DOI: 10.1016/s1359-835x(03)00255-0

Wang, Y., Ren, X., Hou, H., Zhang, Y., and Yan, W. (2015). "Processing and pore structure of aluminium foam sandwich," *Powder Technology* 275, 344-350. DOI: 10.1016/j.powtec.2015.01.066

Yamsaengsung, W., and Sombatsompop, N. (2009). "Effect of chemical blowing agent on cell structure and mechanical properties of EPDM foam, and peel strength and thermal conductivity of wood/NR composite–EPDM foam laminates," *Composites Part B- Engineering* 40(7), 594-600. DOI: 10.1016/j.compositesb.2009.04.003

Article submitted**:** February 2, 2017; Peer review completed**:** June 1, 2017; Revised version received**:** October 8, 2017; Accepted: October 9, 2017; Published: October 11, 2017.
DOI: 10.15376/biores.12.4.9001-9023